Journal of Alloys and Compounds, 207/208 (1994) 33–40
JALCOM 3004

Application of energy upconversion spectroscopy to novel laser and phosphor design

Nigel J. Cockroft
Chemical Science and Technology Division, Mailstop E535, Los Alamos National Laboratory, Los Alamos, NM 87545 (USA)

Abstract

Energy-transfer and sequential-absorption upconversion processes, normally considered detrimental to conventional laser operation, are rapidly emerging as the key to an exciting new class of optical device. Energy-upconversion processes may be designed to take advantage of strong rare earth ion emission transitions in the visible region and of valuable co-incidences with diode-laser outputs in the near-infrared to produce compact visible lasers. This paper reviews the use of sequential-absorption and energy-transfer spectroscopy to derive information that is essential to the optimization of novel device designs as well as 'conventional' laser or phosphor designs. Transfer-rate extraction using upconverted temporal transients, determination of high-lying energy levels using sequential-absorption laser spectroscopy, ion dimer identification by line-narrowing experiments and direct identification of energy storage states using dual-laser techniques are presented. The use of dimer-dominated host crystals, such as $CsCdBr_3$, that can be used to isolate individual energy-transfer rates relevant to the optimization of many different laser types, is emphasized.

1. Introduction

Upon optical illumination of many ion-doped crystals and glasses, several distinct 'energy-upconversion' phenomena may occur which populate highly excited states of optically-active dopant ions. For most traditional laser, amplifier or phosphor device designs, which rely on populating a single low-lying energy state, these phenomena are usually detrimental. Originally motivated by the need to minimize losses in such devices, several single- and dual- laser spectroscopic techniques have been developed to characterize and understand upconversion phenomena. The refinement of these techniques has led to the emergence of a new and exciting field of research that utilizes upconversion phenomena to develop novel optical devices, such as lasers and phosphors, that can operate at shorter wavelengths than their pump sources.

The driving force for the development of such technology is the recent availability of high-powered near-infrared semiconductor-diode lasers and the persistent lack of compact green and blue lasers that are required for high-density optical-data storage, medical therapy, projection applications, and underwater imaging/communication. Energy-upconversion mechanisms are invoked to take advantage of both the strong near-infrared absorptions and the strong visible emission transitions of most lanthanide ions.

This paper reviews, with illustration by specific examples, recent developments in spectroscopy and the application of the four major energy-upconversion mechanisms: sequential absorption, energy transfer, photon avalanche and two-photon absorption.

2. Sequential-absorption upconversion

It is often possible to excite an optical transition from one excited state to another with a transition oscillator strength comparable to, or greater than, the strength of 'normal' transitions from the ground state. Because this process occurs only after the ion has been excited to the initial excited state, this process is referred to as 'sequential absorption' of photons. Although sequential absorption is a loss mechanism referred to as excited-state absorption (ESA) in many traditional lasers, it may also be a useful excitation mechanism for upconversion lasers.

2.1. ESA as a loss mechanism

If the energy separation of highly excited states from the initial state of a desired laser transition coincides with either the wavelength of the optical pump source or with the desired laser output, then ESA can provide a major optical loss for the laser.

SSDI 0925-8388(93)03004-3

The requirement of precise resonance between emission photons and ESA transitions sometimes enables management, by materials design or by nature, of the ESA loss. Laser action in the lanthanide ions, for example, occurs as sharp transitions between manifolds that each comprise several Stark levels. In lasers where the transition with the strongest oscillator strength coincides with an ESA transition, it may be surpassed by weaker transitions between other Stark levels that have no ESA coincidence. This results in unexpected lasing wavelengths and polarizations that may be understood using the sequential-absorption spectroscopies described below. In extreme cases, a given lanthanide ion may not lase at all between certain manifolds in some hosts, but may lase well in an alternative host where the Stark levels have slightly different energies. Sometimes the change required to sufficiently improve the ESA may be as subtle as changing the composition of a glass host [1].

Devices other than lasers are also adversely affected by ESA. Attempts to develop a Nd^{3+} ion-doped optical-fiber amplifier for the 1.3 μm dispersion minimum of silica fiber have been thwarted by strong excited-state absorption at the 1.31 μm wavelength. A search of known glass materials has not yet revealed a host with sufficiently reduced ESA to produce a practical amplifier [2].

2.2. Sequential-absorption upconversion lasers

With careful design, aided by detailed spectroscopy, it is possible to make quite effective short-wavelength lasers that are optically excited by sequential absorption of long-wavelength pump-laser photons. Figure 1 contains a summary of the excitation mechanisms of some laser transitions recently induced by this method. The excitation mechanisms may involve multiple sequential absorption of photons from a single cw pump source, such as the 647 nm excitation of holmium [3] in ZBLAN (fluorozirconate glass) (Fig. 1(a)), or they may involve sequential absorptions at two distinct wavelengths using two cw or pulsed pump lasers such as the 792 nm/840 nm excitation of erbium ions in $YAlO_3$ [4] (Fig. 1(b)). Figure 1(c) demonstrates another good example of two-laser pumping where thulium is excited by both 781 and 649 nm and was used to demonstrate, at Los Alamos National Laboratory, the first blue room temperature energy-upconversion lasing in a bulk crystal (of $YLiF_4$) [6]. A similar mechanism (Fig. 1(d)) was used by an IBM research team to produce the shortest upconversion laser action to date using neodymium ions in $YLiF_4$ [7].

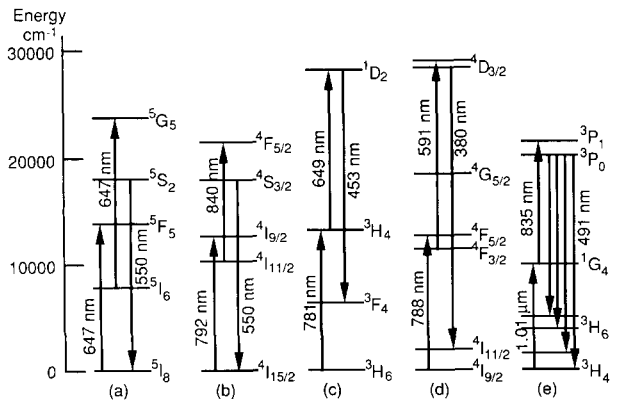

Fig. 1. Several sequential-absorption mechanisms used to induce rare earth upconversion lasing (a) Ho^{3+} [3], (b) Er^{3+} [4], (c) Tm^{3+} [5], (d) Nd^{3+} [7], (e) Pr^{3+} [8].

As the sequential absorption upconversion (SAU) mechanism involves excitation of a single, isolated ion, there is no requirement to have dopant ions in close proximity. A long gain medium with a low dopant concentration is ideal as it reduces losses due to energy-transfer cross-relaxation. Several groups have recently demonstrated that ZBLAN fibers, several meters in length, make ideal gain media for lanthanide-upconversion lasers. For example, Smart *et al.* [8] have demonstrated several visible laser transitions at room temperature for sequential-absorption pumping of praseodymium ions in such fiber (Fig. 1(e)).

2.3. Sequential-absorption spectroscopy

The most versatile probe of sequential absorption processes uses two tunable pulsed lasers. The author and co-workers at Los Alamos National Laboratory use such a system to measure ESA losses for traditional laser design and to design new upconversion lasers [9]. In this system, the spatial and temporal overlap of the two 10-ns pulses can be accurately controlled. The first laser pulse is tuned to an absorption from the ground state. The upconverted emission originating from a high-lying energy state can be monitored while scanning the wavelength of the second laser pulse to provide the ESA excitation spectra. In addition to providing cross-sections of ESA transitions, these spectra will provide the energy level and symmetry label characterization (by polarization dependence) of the upper manifolds. When an appropriate ESA resonance is identified, the emission from high energy states, often not easily pumped by direct means, can be recorded. Similarly, the temporal decay characteristics of a highly excited state can be obtained, and with appropriate modeling, can be used to extract information on the cross-relaxation quenching mechanisms affecting a potential initial laser level [9].

Figure 2 demonstrates the application of sequential-absorption spectroscopy to probe the upper state ($^1D_2$) of the 453 nm Tm^{3+}:$YLiF_4$ upconversion laser transition. The spectrum is obtained by monitoring the $^1D_2$ to $^3H_5$ upconverted emission while scanning the $^3H_4$

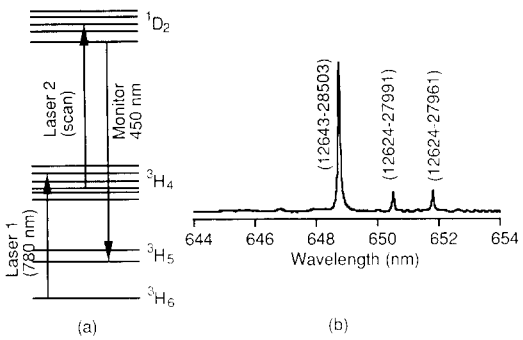

Fig. 2. SAU excitation spectroscopy of the second step of the Tm^{3+}:$YLiF_4$ upconversion laser system (a) excitation mechanism, (b) 75 K excitation spectrum of the $^3H_4$ to $^1D_2$ transitions obtained by monitoring $^1D_2$ to $^3H_5$ emission. $^3H_4$ and $^1D_2$ Stark level energies (in cm^{-1}) are identified in parentheses.

to $^1D_2$ transition (Fig. 1(c)) and the variation of lasing intensity with temporal pulse separation may provide information on the re-equilibration of Stark-level populations in relevant manifolds [5]. The same techniques can be applied with the use of two short wavelength lasers to probe the very high lying energy levels for which no good tunable UV probe source exists [10]. The sequential absorption method offers advantages over direct UV excitation including a reduction of the photo-ionization induced degradation of host matrices.

If two pulsed lasers are not available then a hybrid system using a cw laser (for ground state absorption) and a pulsed laser for ESA can suffice and still provide dynamical information on the upper state through temporal dependence of fluorescence decay.

3 Energy-transfer upconversion

3.1. Types of energy transfer

Unlike the sequential absorption process, which involves the direct excitation of isolated ions with photons, the energy-transfer process involves a non-radiative transfer of energy from an excited ion to a neighbor. This results from a coupling of the multi-poles of ions that are in close proximity. For example, the mechanism for energy transfer between lanthanide ions is often electric dipole-dipole coupling [11].

The macroscopic manifestation of energy transfer depends largely upon the extent of excitation of the recipient ion. Complete energy transfer from an excited ion to an identical, but non-excited, neighbor is a mechanism for energy migration. On the other hand, transfer to a non-identical, non-excited, neighboring ion is the mechanism for sensitization used in many optical phosphors such as those that convert ultraviolet to red radiation by gadolinium to europium energy transfer. A partial transfer of energy to a non-excited neighbor results in both ions populating lower energy states than the state initially excited. This process, called 'cross-relaxation', is always detrimental to laser action if it depopulates, or quenches, the initial state of the laser transition. However, in a few special cases, such as the 2-μm thulium laser where the initial laser level ($^3F_4$) is at half the energy of the pump state level ($^3H_4$), the cross-relaxation process can actually enhance the laser action by efficiently converting ions from the $^3H_4$ pump level to the $^3F_4$ laser level [12].

Energy-transfer upconversion (ETU) is the special case of energy transfer that occurs when an ion that is initially excited receives additional energy from its neighbor. This ion can then fluoresce, or lase, at a wavelength shorter than its pump source. This phenomenon is now being applied by several research groups to the development of an exciting class of lasers and phosphors.

3.2. Energy-transfer upconversion lasers and phosphors

The development of light emitting semiconductor diodes (LEDs) in the 1960s motivated several early studies of phosphors that converted radiation from the near-infrared to the visible by energy transfer upconversion. Auzel [13] and Wright [11] have provided comprehensive reviews of this work that include ytterbium to erbium (green) and ytterbium to thulium (blue) energy transfer in insulating crystals. In 1971, Johnson and Guggenheim [14] demonstrated that such upconversion mechanisms could be used to excite visible laser transitions at low temperatures. Additional progress, motivated by the recent availability of high-power near-infrared diode lasers that are ideal as optical pump sources, was not reported until nearly 15 years later when an IBM team demonstrated 550 nm lasing in erbium-doped $YLiF_4$ for 800 nm excitation [15]. Output powers in excess of 1 W [16] and true diode-laser-pumped lasing [17] have subsequently been reported for this green laser transition. Figure 3 summarizes a few of the upconversion-excitation mechanisms that have resulted in lasing. Particularly significant results include the first mode-locking and Q-switching of a visible upconversion laser [18] (Er^{3+}:$YLiF_4$) and the first demonstration of diode-pumped room-temperature upconversion lasing [19] (Yb^{3+}; Tm^{3+}:BaY_2F_8).

In addition to short wavelength laser transitions, there are some situations where an upconversion excitation mechanism may be used to induce lasing that initiates on a state of higher energy than the pump state but which actually lases at longer wavelength than the pump source. The most well known example is the 2.8 μm transition ($^4I_{11/2}$ to $^4I_{13/2}$) in erbium that is induced by 1.5 μm pumping ($^4I_{15/2}$ to $^4I_{13/2}$) [20] (Fig. 3(b)).

One new research goal for phosphors is the development of materials that can emit three different colors depending on the choice of excitation wavelength.

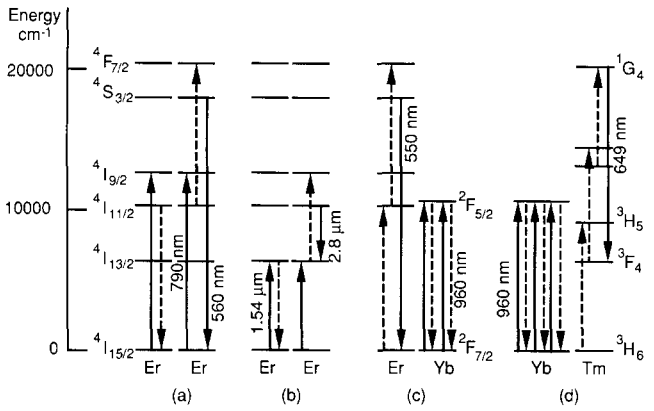

Fig. 3. Several energy-transfer schemes used to induce upconversion lasing. Solid arrows are radiative transitions and dashed lines are non-radiative energy-transfer steps. Figures adapted from the following references: (a) [15–17], (b) [20], (c) [14], (d) [19].

This was recently demonstrated for erbium in $CsCdBr_3$ which emits at 493 nm, 414 nm or 651 nm for 984 nm, 801 nm or the 984 nm/801 nm combination, respectively [21]. If the chromaticity coordinates can be modified, such phosphors may be appropriate for projection applications where diode lasers are focused onto a phosphor-coated screen.

3.3. ETU spectroscopy

A system comprising one or two tunable-pulsed lasers provides a very versatile experimental capability for probing ETU phenomena.

3.3.1. Single-laser probe experiments

3.3.1.1. Fluorescence, pump power, and temperature dependencies. Observation and assignment of short wavelength emission features upon longer wavelength laser excitation is the most simple verification of energy upconversion. The variation in intensity of upconverted fluorescence with the pump power, or energy, is often the next step towards identifying the mechanism. If no saturation occurs, quadratic, cubic or quartic dependence of output power with input power will generally indicate the conversion of 2, 3 or 4 pump quanta, respectively, by the upconversion process.

Unlike sequential-absorption upconversion, which requires exact overlap of pump photon energy and the ESA transitions, ETU processes can involve mismatches between the donor and acceptor energies. These mismatches are accommodated by the absorption or creation of lattice phonons which may be investigated by characterizing the variation of emission intensity with sample temperature. Although not specifically applied to ETU studies to date, a summary of these techniques applied to other types of non-upconversion energy transfer is given in ref. [22].

3.3.1.2. Temporal decay measurements. Since the transfer of energy from an excited ion to its equally excited neighbor depletes the population of that excited state, a quenching of the lifetime of the state is observed. Conversely, the same process acts as a population feeding term for the highly excited state that decays to give the short wavelength emission. Energy transfer rates must therefore be extracted from the measurement and analysis of temporal decays of fluorescence from several relevant excited states. The most distinguishing feature of ETU compared to SAU emission is the form of the temporal decay. SAU emission will typically appear as a simple exponential decay resembling that observed for direct upper-state excitation. ETU emission, however, will generally exhibit long rise and decay times that reflect the long lifetimes of the intermediate states involved in the process [21]. The form of the transient will therefore depend strongly on the excitation pathway. For example, Fig. 4 shows the $^4S_{3/2}$ to $^4I_{15/2}$ (560 nm) emission decay of erbium in Y_2O_3. The directly excited (green pump) decay time of 92 μs is significantly faster than that obtained by red pumped ($^4F_{9/2}$) ETU or by near-infrared pumped ($^4I_{9/2}$) ETU.

Although the theory of energy transfer processes has been quite well developed by Dextor [23], Forster [24] and subsequent workers [25], the precise experimental determination of energy transfer parameters has been notoriously difficult for most materials. The root cause of the difficulty is the inherent superposition of multiple rates, resulting from several possible ion separations, present in most observables such as fluorescence decay curves. A typical transient that is quenched by energy transfer exhibits fast initial decay which slows to a constant rate at longer times [22]. An effective decay rate must be deconvoluted from the form of the decay transient by assuming a model for the distribution of dopant ions and for the coupling mechanism involved. Models formulated by Inokuti and Hirayama [26] are often invoked for this purpose.

Recently it has been demonstrated that a special class of materials are particularly useful for probing

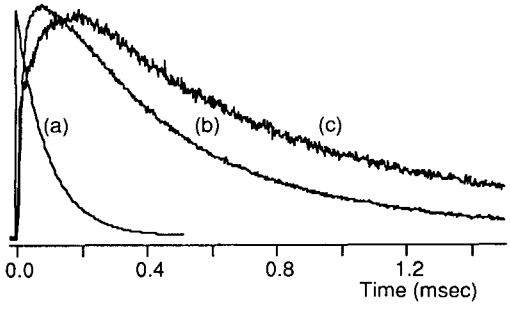

Fig. 4. $^4S_{3/2}$ to $^4I_{15/2}$ (563 nm) emission transients at 10 K for 1% Er^{3+}:Y_2O_3 after: (a) $^4S_{3/2}$ (direct) excitation, (b) $^4F_{9/2}$ (red) excitation, (c) $^4I_{9/2}$ (near-infrared) excitation.

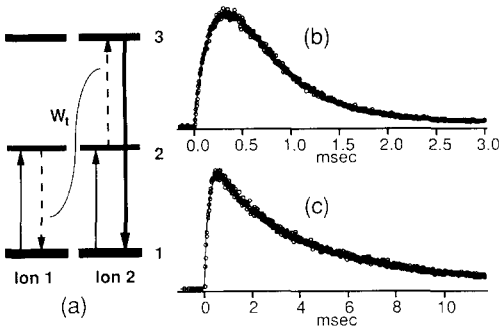

Fig. 5. Erbium-dimer upconversion in $CsCdBr_3$ at 10 K (adapted from ref. [21]). Solid line fits assume single-transfer rate model. (a) General model for three-level system, (b) levels 1, 2, 3 are $^4I_{15/2}$, $^4I_{9/2}$, $^2H_{9/2}$, respectively, (c) levels 1, 2, 3 are $^4I_{15/2}$, $^4I_{11/2}$, $^4F_{7/2}$, respectively.

ETU transfer rates. $CsCdBr_3$, and related compounds, accommodate trivalent ions in a single dimer center with a constant ion separation [27]. For example, three divalent cadmium ions will be replaced by two trivalent erbium ions located 6 Å apart and separated by a cadmium ion vacancy. When both ions of the dimers are excited by a near-infrared laser, they undergo efficient ETU [21]. Figure 5(a) represents a generalized energy transfer process in which two ions in state 2 exchange energy to leave one in state 3 and one in state 1. For materials such as $CsCdBr_3$, it is possible to solve the population rate equations exactly by assuming a single transfer rate W_t and by considering the population, N_d, of doubly excited dimers [21]. The solution for the population decay of level 3 is therefore

$$N_3 = \frac{N_d^0 W_t}{[W_3 - (2W_2 + W_t)]} (e^{-(2W_2 + W_t)t} - e^{-W_3 t}) \qquad (1)$$

where N_d^0 is the initial population of doubly excited dimers, W_t is the ETU rate, and W_2 and W_3 are the intrinsic decay rates for levels 2 and 3, respectively. Upconverted fluorescent transients for level 3 can therefore be fitted to an intensity expression representing a superposition of an exponential rise and decay.

Figure 5 shows the excellent quality of such fits for the case of erbium ETU where the labels 1, 2 and 3 correspond to the $^4I_{15/2}$, $^4I_{9/2}$ and $^2H_{9/2}$ manifolds (Fig. 5(b)) and to the $^4I_{15/2}$, $^4I_{11/2}$ and $^4F_{7/2}$ manifolds (Fig. 5(c)), respectively. Thus, using such dimer-dominated compounds, direct comparisons can be made of the efficiencies of different ETU processes. The ETU rate extracted from Fig. 5(b), for example, is 13.6 times greater than the 128 s^{-1} rate of the process in Fig. 5(c) [21]. This information is essential to the design of new upconversion lasers.

3.3.1.3. Line narrowed excitation spectroscopy. Site selective excitation using a single tunable pulsed laser can sometimes be used to extract ETU information

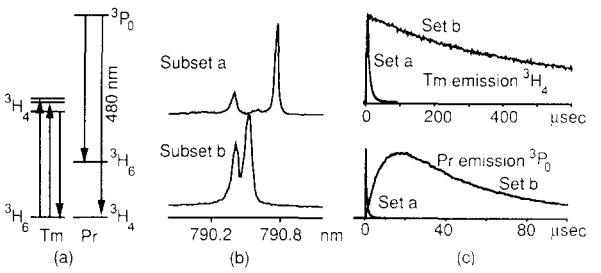

Fig. 6. Site-selective upconversion in Tm^{3+}/Pr^{3+} co-doped $YLiF_4$ at 10 K. (a) Excitation/emission scheme, (b) near-infrared $^3H_6$ to $^3H_4$ (Tm^{3+}) excitation spectra monitoring blue $^3P_0$ to $^3H_4$ (Pr^{3+}) emission for two different subsets of Tm/Pr ions, (c) variation in temporal decay of emission for the two Tm/Pr subsets.

about dopants in a 'typical' laser host, such as $YLiF_4$, which exhibits a distribution of dopant ion separations. A comparison of laser excitation scans obtained by monitoring upconverted fluorescence with those obtained by monitoring 'Stokes' fluorescence often reveals that the former have relatively narrow transitions located to the side of the central absorption peaks. For example, in the upconversion laser material Tm, Yb:BaY_2F_8, we have observed that the linewidth at 10 K of the 971 nm Yb^{3+} excitation transition is reduced by a factor of 9.3 when upconverted Tm^{3+} emission (480 nm) is monitored rather than the Yb^{3+} emission. This line-narrowing effect is due to the preferential excitation of subsets of dopant ions that have a smaller-than-average ionic separation.

Detailed comparison of upconverted transients as a function of excitation wavelength can enable further de-convolution of ion dimer and trimer subsets. Figure 6 demonstrates an extreme example of this effect where $^3P_0$ to $^3H_4$ emission (480 nm) from praseodymium ions is observed when thulium $^3H_6$ to $^3H_4$ (790 nm) transitions are excited in doubly doped $YLiF_4$. The large perturbation of Tm^{3+} ion levels (shown as a large transition splitting for subset a in Fig. 6(b)) is due to the field of a very nearby Pr^{3+} ion. This subset has very fast rise and decay rates (Fig. 6(c)) and strong upconversion emission (intensity not to scale on the plots). The slower emission rise and decay rates and smaller Stark splittings of subset b are consistent with a greater Tm^{3+}-Pr^{3+} ion separation.

3.3.2. Dual-laser probe experiments

The availability of a second tunable, pulsed laser enhances the ability to spectroscopically extract information on ETU processes. Although not widely used to date, the dual laser techniques are valuable for identifying intermediate states that are involved in multiple-step energy transfer pathways.

Dimer-dominated materials, such as $CsCdBr_3$, are ideal hosts for demonstrating the utility of dual laser techniques since energy transfer can be controlled and

restricted to the two ions of a dimer [21]. If the material is doped with two different types of ions, say A and B, a good fraction of the dopants will form heterogeneous A–B dimers. The energy transfer steps involved in ion combinations such as Yb–Tm, Yb–Er, Nd–Cr, Tm–Ho that are used in practical laser systems could be isolated and investigated independently.

The following experiments are representative of the approach that we have used to examine energy transfer in Tm^{3+}/Pr^{3+} ion dimers, the details of which will be reported elsewhere. The methods, illustrated in Fig. 7, are applicable to the study of any multiple transfer step A–B dimer. A laser pulse resonant with a ground state absorption of ion A is used to excite the A ions of the A–B dimers. This energy may decay radiatively or non-radiatively on ion A or, more importantly, it may be transferred to ion B. Four different experiments, shown in Fig. 7, may then be performed using a second laser: (a) A second pulse of the same wavelength can be supplied to ion A. If an energy-transfer upconversion resonance exists, this excitation may then transfer from ion A to ion B in a second step that promotes the partially excited ion B to a higher energy level (Fig. 7(a)). The dependence of the upconverted fluorescence intensity, from the high energy state of ion B, on the temporal delay between the two laser pulses will provide the lifetime, and therefore the identity, of the intermediate state of ion B that is involved in the ETU process. (b) After the first pulse is absorbed by ion A, the second laser pulse can be tuned to ESA transitions of ion B (Fig. 7(b)). If a particular level of ion B is receiving and storing energy from ion A, it is possible to observe upconverted emission from ion B when an ESA transition that originates on that level is excited. This technique provides verification of the importance of different possible intermediate states of ion B that may contribute to the ETU process. (c) Experiments (a) and (b) may also be performed while monitoring the temporal transient of the emission from the suspected intermediate state, rather than the upconverted state, of ion B. At the moment of the second pulse, the fluorescence intensity of the ion B emission will exhibit a rapid decrease as the intermediate state is depopulated by the ETU or ESA step. Such an observation provides the most direct verification of the intermediate pathways of ETU processes. Figure 8 shows an experiment of this type. The figure shows the emission decay of the $^1G_4$ level of Pr^{3+} (1.02 μm) after pulsed excitation of the $^3H_4$ level of Tm^{3+} (799 nm) in Tm–Pr dimers in $CsCdBr_3$. The dramatic dip in the intensity around 1 ms is due to depletion of the state by a second 10 ns laser pulse tuned to the Pr^{3+} $^1G_4$ to $^3P_2$ (804 nm) ESA transition (Fig. 7(b)). (d) If a particular two-step ETU pathway is suspected, the second step can be isolated by initially exciting ion B to the suspected intermediate state and using a second laser pulse to excite ion A (Fig. 7(c)). Upconversion emission from ion B will be observed if the energy from ion A is transferred to ion B by the second step of the ETU process. This method effectively bypasses the first step of the ETU process and analysis of the temporal decay of the upconversion fluorescence enables the extraction of the ETU rates for the second step.

A fifth type of upconversion spectroscopy is possible using two pulsed lasers. Erbium ion dimers in $CsCdBr_3$ can be heterogeneously excited by two simultaneous laser pulses tuned to 984 nm and 801 nm that will excite one ion in the dimer to the $^4I_{11/2}$ manifold and one to the $^4I_{9/2}$ manifold. An ETU process then occurs that populates the $^4F_{5/2}$ manifold that has approximately the energy of the sum of the $^4I_{9/2}$ and $^4I_{11/2}$ manifolds. Strong red ($^4F_{5/2}$ to $^4I_{13/2}$) emission occurs due to this process [21]. This double-pumped excitation mechanism has potential for application to a new type of multicolor upconversion laser and phosphor.

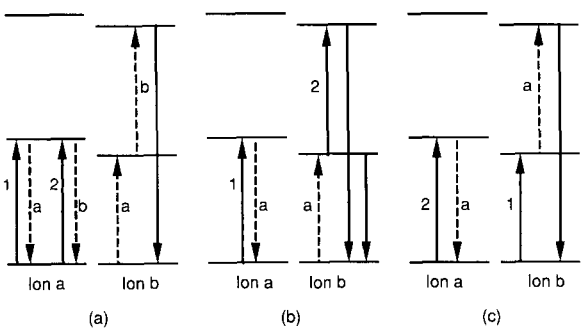

Fig. 7. Generalized dual-laser ETU spectroscopy techniques. Laser pulses (solid arrows) are numbered sequentially and non-radiative energy transfer steps are labeled 'a' or 'b'. (a) Two-pulse probe of energy transfer, (b) intermediate state verification by ESA, (c) bypassing of the first ETU step.

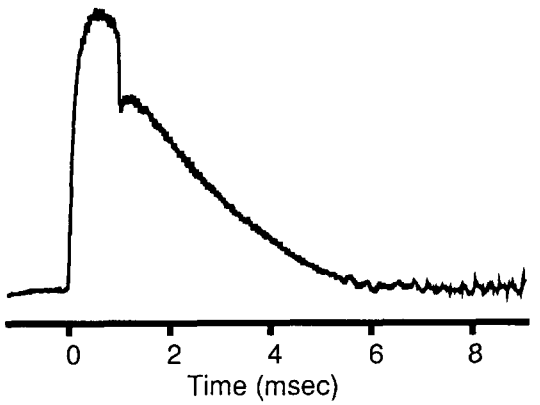

Fig. 8. $^1G_4$ to $^3H_4$ (Pr^{3+}) emission (1.02 μm) decay in $CsCdBr_3$ after 799 nm $^3H_6$ to $^3H_4$ (Tm^{3+}) excitation at 10 K. A $^1G_4$ to $^3P_2$ (Pr^{3+}) ESA laser pulse (804 nm), incident 1 ms after the thulium excitation pulse, depletes the population of $^1G_4$.

3.4. Other types of upconversion spectroscopy

Several lanthanide ions have exhibited a 'photon avalanche' effect which is a hybrid of the ESA and energy-transfer phenomena. The ions are excited with a cw laser resonant with an ESA transition that originates several thousand wavenumbers above the ground state. The terminating state of the ESA transition then decays, by energy transfer to a non-excited neighbor, to leave both ions in the initial state of the ESA transition. The population in the latter therefore grows rapidly until a laser threshold is reached. The best examples of avalanche lasing or spectroscopy have been demonstrated using praseodymium [28] and thulium [29] ion-doped systems.

Although occasionally used to identify high lying energy levels, two-photon absorption (TPA) where the laser pump is not resonant with a real absorption level, is not normally an effective upconversion-excitation mechanism. In fact, Auzel [30] has determined that TPA is usually ten orders of magnitude weaker than ETU. Nevertheless, we have observed an interesting result, in erbium-doped $YScO_3$, that is consistent with being a possible exception to this trend. This material has one Er^{3+} ion center with C_2 symmetry and one with C_{3i} symmetry. Because of its inversion symmetry, the latter center does not allow the normally dominant electric dipole-dipole single-photon transitions. We have observed, however, efficient upconverted emission from the C_2 center when exciting a wavelength ($\sim$813 nm) that appears to match the two-photon absorption to the $^2H_{9/2}$ manifold of the C_{3i} center. This energy must then be transferred to the C_2 center from which emission is observed. The efficiency of this process appears to be within an order-of-magnitude of that for direct ETU. excitation (*via* $^4I_{9/2}$ absorption) of the C_2 center. Details and confirmation of this effect will be published elsewhere.

4. Conclusions

Whether viewed as detrimental or essential in a given situation, energy-upconversion phenomena are now recognized as being integral to most optical devices. Recently, laser-based spectroscopies have been developed which are used to obtain parameters that will optimize or minimize the phenomena. The excitation spectra using single or dual laser experiments can be used to identify the resonances involved in ESA and ETU processes. Fits to temporal decays of upconverted fluorescence enable extraction of the energy transfer rates. If a second laser is used, it is often possible to identify the intermediate energy states and to isolate the energy transfer rates in multiple-step ETU processes. This type of information is critical to the design of novel devices that utilize energy-upconversion effects.

Acknowledgments

Some of the results described are due to collaborations with others including Keith Murdoch, University of Canterbury (Tm–Pr transfer), Brian Tissue, Los Alamos National Laboratory (L.A.N.L.) ($YScO_3$ upconversion), and Dinh Nguyen, L.A.N.L. (Yb–Tm transfer). Technical assistance for several experiments was provided by George Faulkner (L.A.N.L.).

References

1 P.R. Morkel, M.C. Farris and S.B. Poole, *Opt. Commun., 67* (1988) 349.
2 M. Brierley, *Opt. Photonics News, Jan.* (1992) 14.
3 J.Y. Allain, M. Monerie and H. Poignant, *Electronics Lett., 26* (1990) 261.
4 A.J. Silversmith, W. Lenth and R.M. Macfarlane, *Appl. Phys. Lett., 51* (1987) 1977.
5 D.C. Nguyen, G.E. Faulkner and M. Dulick, *Appl. Opt., 28* (1989) 3553.
6 D.C. Nguyen, G.E. Faulkner, M.E. Weber and M. Dulick, *Proc. SPIE, Solid State Lasers*, Vol. 1223, SPIE, 1990, p. 54.
7 R.M. Macfarlane, F. Tong, A.J. Silversmith and W. Lenth, *Appl. Phys. Lett., 52* (1988)1300.
8 R.G. Smart, D.C. Hanna, A.C. Tropper, S.T. Davey, S.F. Carter and D. Szebesta, *Electron. Lett., 27* (1991)1307 .
9 M. Dulick, G.E. Faulkner, N.J. Cockroft and D.C. Nguyen, *J. Lumin., 48* (1991) 517.
10 C.G. Levey, T.J. Glynn and W.M. Yen, *J. Lumin., 31* (1984) 245.
11 J.C. Wright, in F.K. Fong (ed.), *Radiationless Processes in Molecules and Condensed Phases*, Vol 15, Springer-Verlag, Berlin, 1976, Ch. 4.
12 R.C. Stoneman and L. Esterowitz, *Opt. Lett., 15* (1990) 486.
13 F.E. Auzel, *Proc. IEEE, 61* (1973) 753.
14 L.F. Johnson and H.J. Guggenheim, *Appl. Phys. Lett., 19* (1971) 44.
15 W. Lenth, A.J. Silversmith and R.M. Macfarlane, in A.C. Tam, J.L. Gole and W.C. Stawalley (eds.), *Advances in Laser Sciences III*, Atlantic City NJ, 1987, AIP Conf. Proc. No. 172, 1988, pp. 8–12.
16 G.C. Valley and R.A. McFarlane, in L.L. Chase and A.A. Pinto (eds.), *OSA Proc. on Advanced Solid-State Lasers*, Vol 13, 1992, p. 376.
17 F. Tong, W.P. Risk, R.M. Macfarlane and W. Lenth, *Electron. Lett., 25* (1989) 1389.
18 P. Xie and S.C. Rand, *Opt. Lett., 17* (1992) 1116.
19 R.J. Thrash and L.F. Johnson, *OSA Annual Meeting*, Albuquerque, USA , 1992, Paper MJ1.
20 S.A. Pollack, D.B. Chang and N.L. Moise, *J. Appl. Phys., 60* (1986) 4077.
21 N.J. Cockroft, G.D. Jones and D.C. Nguyen, *Phys. Rev. B, 45* (1992) 5187.
22 W.M. Yen, in A.A. Kaplyanskii and R.M. Macfarlane (eds.), *Spectroscopy of Solids Containing Rare Earth Ions*, Elsevier, Amsterdam, 1987, Ch. 4.

23 D.L. Dexter, *J. Chem. Phys., 21* (1953) 836.
24 T. Forster, *Naturwissenschaften, 33* (1946) 166.
25 H.C. Chow and R.C. Powell, *Phys. Rev. B., 21* (1980) 3785.
26 M. Inokuti and F. Hirayama, *J. Chem. Phys., 43* (1965) 1978.
27 L.M. Henling and G.L. McPherson, *Phys. Rev. B., 16* (1977) 4756.
28 M.E. Koch, A.W. Kueny and W.E. Case, *Appl. Phys. Lett., 56* (1990) 1083.
29 H. Ni and S.C. Rand, *Opt. Lett., 16* (1991) 1424.
30 F.E. Auzel, private communication.